12-11-2004

A Comparative Analysis of Proportional-Integral Compensated Shunt Active Power Filters

Matthew Alan Gray

A COMPARATIVE ANALYSIS OF PROPORTIONAL-INTEGRAL COMPENSATED AND SLIDING MODE COMPENSATED SHUNT ACTIVE POWER FILTERS

By

Matthew Alan Gray

A Thesis
Submitted to the Faculty of
Mississippi State University
in Partial Fulfillment of the Requirements
for the Degree of Master of Science
in Electrical Engineering
in the Department of Electrical and Computer Engineering

Mississippi State, Mississippi

December 2004

A COMPARATIVE ANALYSIS OF PROPORTIONAL-INTEGRAL

COMPENSATED AND SLIDING MODE

COMPENSATED SHUNT ACTIVE

POWER FILTERS

By

Matthew Alan Gray

Approved:

_____	_____
Dr. Randolph Follet, P.E. (Director of Thesis)	Dr. Nick Younan Graduate Coordinator of the Department of Electrical and Computer Engineering
_____	
Dr. Herb Ginn (Committee Member)	
_____	_____
Dr. James Harden (Committee Member)	Dr. Glenn Steele Interim Dean of the College of Engineering

Name: Matthew Alan Gray

Date of Degree: December 10, 2004

Institution: Mississippi State University

Major Field: Electrical Engineering

Major Professor: Dr. Randolph Follett, P.E.

Title of Study: A COMPARATIVE ANALYSIS OF PROPORTIONAL-INTEGRAL COMPENSATED AND SLIDING MODE COMPENSATED SHUNT ACTIVE POWER FILTERS

Pages in Study: 47

Candidate for Degree of Master of Science

This thesis deals primarily with the simulation and analysis of shunt active power filters (APF) on a three-phase power distribution system possessing a harmonic generating load. The shunt active power filters are analyzed based on effective total harmonic distortion (THD) levels and response to changing dynamics. These results are derived from the simulation of a pulse-width modulation (PWM) controlled voltage source inverter (VSI) with a capacitor connected to the DC side of the VSI. The primary difference between individual simulations is the particular control law implemented in the shunt APF.

TABLE OF CONTENTS

LIST OF TABLES

LIST OF FIGURES

CHAPTER I

INTRODUCTION

Overview

This thesis addresses the comparison and analysis of shunt active power filtering schemes with differing control laws. A comprehensive analysis of the theory behind the operation of a VSI shunt active power filter is presented, including a theoretical analysis of both proportional-integral and sliding mode control laws. Simulation results of both methods are also presented, providing information on performance and response to changing dynamics.

The remainder of this chapter is organized as follows: first, the motivation for the simulations is presented in Section 1.2. The goals and contributions of this work are summarized in Section 1.3. The organization of the rest of this thesis is outlined in Section 1.4.

Motivation

The extensive use of nonlinear loads in power distribution systems gives rise to often undesirable, and sometimes damaging, voltage and current harmonics. These harmonics can be sufficiently attenuated through both passive and active power filtering techniques. Active power filtering techniques, while being more robust than passive techniques, are also more complex.

In conjunction with research related to the simulation and implementation of power distribution systems on naval vessels, consideration of various harmonic power filtering schemes were executed, of which active power filtering techniques were one of these considerations. Thus, simulation of said techniques became necessary to sufficiently explore this option.

Goals and Contributions

The primary goal of this thesis is to provide a comparative analysis of active power filtering techniques with proportional-integral and sliding mode control laws.

Organization

The remainder of this thesis is arranged in the following four sections: a brief introduction to active power filtering techniques, an analysis of the theory of operation of an active power filter and compensation techniques, an evaluation of simulations and their results, a brief discussion of caveats in implementation, and a summary and conclusion of findings.

CHAPTER II

A BRIEF INTRODUCTION TO ACTIVE POWER FILTERING

Harmonic contamination can be a significant contributor to power losses in AC lines [2,3,4]. Conventional solutions to this problem consist of passive resonant harmonic filtering techniques; however, such techniques are incapable of compensating for unpredictable harmonic events and are subject to uncontrollable environmental parameters [4,6,13,15]. Therefore, active filtering solutions that are capable of dynamic cancellation of randomly occurring harmonic phenomena are attractive alternatives [2,3,4,7].

There are two distinct classifications of active power filters: series (inductive), and shunt (capacitive). However, it is conceivable to design hybrid solutions consisting of a series active power filter, a shunt active power filter, or both, as well as traditional passive filtering components [5]. The focus in this thesis is on shunt filtering technologies.

Shunt passive power filters, commonly referred to as LC filters or resonant harmonic filters, are a conventional solution to eliminating harmonic distortion in a power distribution system. However, these types of filters are incapable of accommodating highly transient conditions where the distortion present in a system is unpredictable [6, 13, 15].

Shunt active power filters, as their name implies, are connected in parallel with a harmonic generating load. They are normally used to compensate current harmonic distortion. The most common configuration of a shunt active power filter is that of a three-leg voltage

source inverter connected to a three-phase power distribution system with a DC capacitor connected to the DC side of the inverter. Using appropriate current sensors, this type of active power filter normally isolates unwanted current harmonics from the fundamental harmonic in the load current and cancels them out by injecting these same harmonics phase shifted by 180 degrees [2,3,6]. This injected current is produced through some form of pulse-width modulation applied to the gate terminals of the FETs or IGBTs of the voltage source inverter. Common modulation methods include sinusoidal modulation and space vector modulation [13,18,19,21].

The compensation methods discussed in this thesis involve a variation on the proportional-integral compensation method described by N. Mendalek and K. Al-Haddad in [2] and a sliding mode compensation method described by N. Mendalek, K. Al-Haddad, F. Fnaiech, and L.A. Dessaint in [3]. Both shunt active power filter solutions serve to compensate unwanted current harmonics out of a power distribution system.

CHAPTER III

THEORY OF OPERATION OF AN ACTIVE POWER FILTER

The model of a power distribution system with a shunt active power filter can be seen in Figure 1.1.

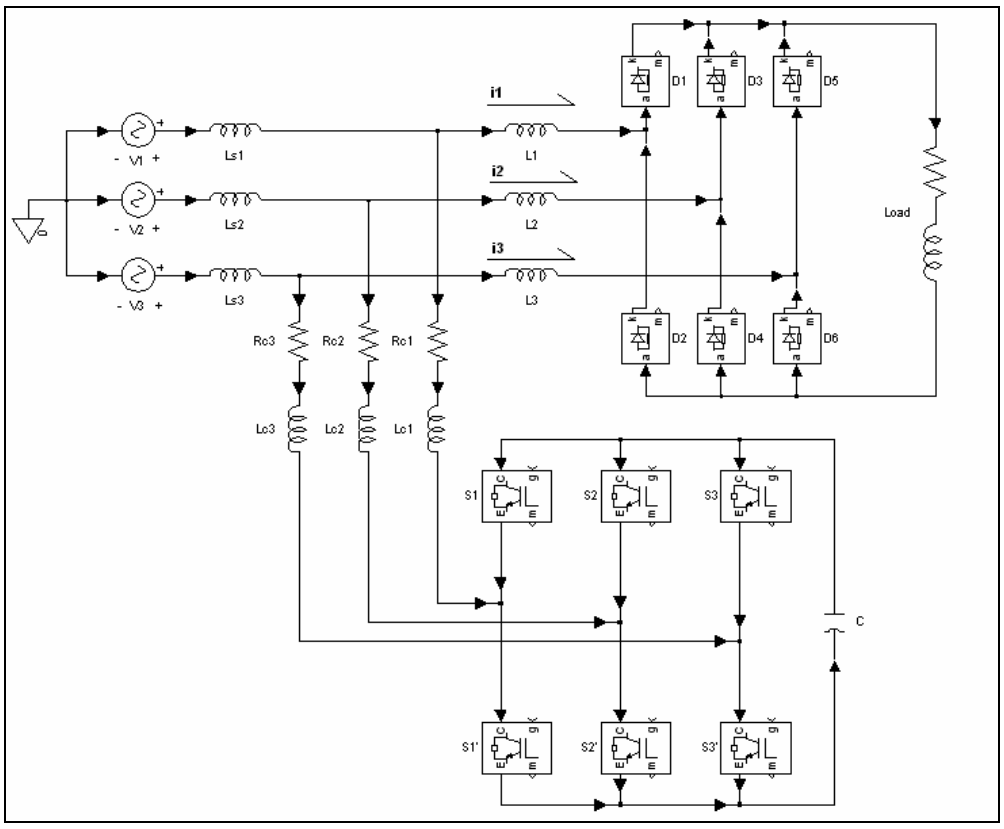

Figure 1.1 – Model of a Power Distribution System with a Shunt APF

As can be seen, a common active power filter as it is applied to a three-phase power distribution system consists of a three-branch voltage source inverter (VSI) with a capacitor connected to the DC side of the VSI, a common component of most active power filter topologies [8,9,10,12,17,18,19,20].

Kirchoff's rules for voltages and currents as applied to this system provide us with the three differential equations in the stationary abc frame

$$\begin{aligned} v_1 &= L_c \frac{di_1}{dt} + R_c i_1 + v_{1M} + v_{MN} \\ v_2 &= L_c \frac{di_2}{dt} + R_c i_2 + v_{2M} + v_{MN} \\ v_3 &= L_c \frac{di_3}{dt} + R_c i_3 + v_{3M} + v_{MN} \end{aligned} \tag{3-1}$$

Using the following assumptions

$$\begin{aligned} v_1 + v_2 + v_3 &= 0 \\ i_1 + i_2 + i_3 &= 0 \end{aligned} ,$$

we arrive at the following

$$v_{MN} = -\frac{1}{3}\sum_{m=1}^{3} v_{mM} \tag{3-2}$$

The switching function of c_k of the k^{th} leg of the converter is

$$c_k = \begin{cases} 1, \textit{ if } S_k \textit{ is on and } S_k' \textit{ is off} \\ 0, \textit{ if } S_k \textit{ is off and } S_k' \textit{ is on} \end{cases} \tag{3-3}$$

Thus, $v_{kM} = c_k v_{dc}$. This gives

$$\frac{di_k}{dt} = \frac{R_c}{L_c} i_k - \frac{1}{L_c}(c_k - \frac{1}{3}\sum_{m=1}^{3} c_m) v_{dc} + \frac{v_k}{L_c} \tag{3-4}$$

A switching state function is defined as

$$d_{nk} = (c_k - \frac{1}{3}\sum_{m=1}^{3} c_m)_n \tag{3-5}$$

Conversion from $[c_k]$ to $[d_{nk}]$ is given by the relation

$$\begin{bmatrix} d_{n1} \\ d_{n2} \\ d_{n3} \end{bmatrix} = \frac{1}{3}\begin{bmatrix} 2 & -1 & -1 \\ -1 & 2 & -1 \\ -1 & -1 & 2 \end{bmatrix}\begin{bmatrix} c_1 \\ c_2 \\ c_3 \end{bmatrix} \tag{3-6}$$

Note that the transformation matrix is of rank 2 and $[d_{nk}]$ has no zero sequence component (i.e. $d_{n1} + d_{n2} + d_{n3} = 0$).

Analysis of the DC component of the system gives

$$\frac{dv_{dc}}{dt} = \frac{1}{C} i_{dc} = \frac{1}{C}\sum_{m=1}^{3} c_m i_m$$

It can be shown that

$$\sum_{m=1}^{3} d_{nm} i_m = \sum_{m=1}^{3} c_m i_m \ ,$$

allowing us to arrive at the following

$$\frac{dv_{dc}}{dt} = \frac{1}{C}\sum_{m=1}^{3} d_{nm} i_m \ . \tag{3-7}$$

With the absence of zero-sequence components in $[i_k]$ and $[d_{nk}]$, we get

$$\frac{dv_{dc}}{dt} = \frac{1}{C}(2d_{n1} + d_{n2})i_1 + \frac{1}{C}(d_{n1} + 2d_{n2})i_2 \tag{3-8}$$

The complete model of the active filter in the stationary abc frame is

$$\frac{d}{dt}\begin{bmatrix} i_1 \\ i_2 \\ v_{dc} \end{bmatrix} = \begin{bmatrix} -\frac{R_c}{L_c} & 0 & -\frac{d_{n1}}{L_c} \\ 0 & -\frac{R_c}{L_c} & -\frac{d_{n2}}{L_c} \\ \frac{2d_{n1}+d_{n2}}{C} & \frac{d_{n1}+2d_{n2}}{C} & 0 \end{bmatrix}\begin{bmatrix} i_1 \\ i_2 \\ i_3 \end{bmatrix} + \frac{1}{L_c}\begin{bmatrix} v_1 \\ v_2 \\ 0 \end{bmatrix} \tag{3-9}$$

Since the steady-state fundamental components are sinusoidal, the system is transformed into the synchronous orthogonal frame rotating at the supply frequency, ω.

$$C_{dq0}^{123} = \sqrt{\frac{2}{3}}\begin{bmatrix} \cos\theta & \cos(\theta-\frac{2\pi}{3}) & \cos(\theta-\frac{4\pi}{3}) \\ -\sin\theta & -\sin(\theta-\frac{2\pi}{3}) & -\sin(\theta-\frac{4\pi}{3}) \\ \frac{1}{\sqrt{2}} & \frac{1}{\sqrt{2}} & \frac{1}{\sqrt{2}} \end{bmatrix} \tag{3-10}$$

Where $\theta = \omega t$, and $C_{dq0}^{123} = (C_{dq0}^{123})^{-1} = (C_{dq0}^{123})^{T}$

Equation (3-7) can be rewritten as:

$$\frac{dv_{dc}}{dt} = \frac{1}{C}\left[d_{n123}\right]^{T}\left[i_{123}\right] \tag{3-11}$$

Applying the coordinate transformation, we get

$$\frac{dv_{dc}}{dt} = \frac{1}{C}\left(C_{123}^{dq0}\left[d_{ndq0}\right]\right)^{T}\left(C_{123}^{dq0}\left[i_{dq0}\right]\right) = \frac{1}{C}\left[d_{ndq0}\right]^{T}\left[i_{dq0}\right]$$

With the zero-sequence in $\left[d_{ndq0}\right]$ and $\left[i_{dq0}\right]$ being negligible, we can assume that

$$\frac{dv_{dc}}{dt} = \frac{d_{nd}i_d}{C} + \frac{d_{nq}i_q}{C} \tag{3-12}$$

Similarly, the following can be derived

$$\frac{d}{dt}\left[i_{123}\right] = -\frac{R_c}{L_c}\begin{bmatrix} 1 & 0 & 0 \\ 0 & 1 & 0 \\ 0 & 0 & 1 \end{bmatrix}\left[i_{123}\right] - \frac{1}{L_c}\left[d_{n123}\right]v_{dc} + \frac{1}{L_c}\left[v_{123}\right], \tag{3-13}$$

which can be transformed into

$$\frac{d}{dt}\left[i_{dq0}\right]=-\begin{bmatrix}\frac{R_c}{L_c} & -\omega & 0\\ \omega & \frac{R_c}{L_c} & \omega\\ 0 & -\omega & \frac{R_c}{L_c}\end{bmatrix}\left[i_{dq0}\right]-\frac{1}{L_c}\left[d_{ndq0}\right]v_{dc}+\frac{1}{L_c}\left[v_{dq0}\right] \tag{3-14}$$

The resulting transformed model in the synchronous orthogonal rotating frame is as follows

$$\frac{d}{dt}\begin{bmatrix}i_d\\ i_q\\ v_{dc}\end{bmatrix}=\begin{bmatrix}-\frac{R_c}{L_c} & \omega & -\frac{d_{nd}}{L_c}\\ -\omega & -\frac{R_c}{L_c} & -\frac{d_{nq}}{L_c}\\ \frac{d_{nd}}{C} & \frac{d_{nq}}{C} & 0\end{bmatrix}\begin{bmatrix}i_d\\ i_q\\ v_{dc}\end{bmatrix}+\frac{1}{L_c}\begin{bmatrix}v_d\\ v_q\\ 0\end{bmatrix} \tag{3-15}$$

which can also be rewritten as

$$\frac{d}{dt}\begin{bmatrix}i_d\\ i_q\\ v_{dc}\end{bmatrix}=\begin{bmatrix}-\frac{R_c}{L_c} & \omega & 0\\ -\omega & -\frac{R_c}{L_c} & 0\\ 0 & 0 & 0\end{bmatrix}\begin{bmatrix}i_d\\ i_q\\ v_{dc}\end{bmatrix}+\begin{bmatrix}-\frac{v_{dc}}{L_c} & 0\\ 0 & -\frac{v_{dc}}{L_c}\\ \frac{i_d}{C} & \frac{i_q}{C}\end{bmatrix}\begin{bmatrix}u_1\\ u_2\end{bmatrix}+\begin{bmatrix}\frac{v_d}{L_c}\\ \frac{v_q}{L_c}\\ 0\end{bmatrix} \tag{3-16}$$

where $u_1 = d_{nd}$ and $u_2 = d_{nq}$.

CHAPTER IV

PI COMPENSATION OF AN ACTIVE POWER FILTER

A proportional-integral control law was derived through linearization of the inherently nonlinear active power filter system model, in effect decoupling the tasks of harmonic current tracking and DC capacitor voltage regulation. This decoupling allows us to compensate the currents and the capacitor voltage independently of each other, providing that either one or the other of these decoupled systems has a system response significantly less than the other.

Harmonic Current Control

Since it is conceivable that the current control law should be able to track (and therefore compensate) high-order harmonics, we choose the current control law to have a faster system response than the DC voltage control law. This being said, an analysis of the environment the current control law will be regulating is described by the following two equations derived from the model in (15):

$$\begin{aligned} L_c \frac{di_d}{dt} + R_c i_d &= L_c \omega i_q - v_{dc} d_{nd} + v_d \\ L_c \frac{di_q}{dt} + R_c i_q &= -L_c \omega i_d - v_{dc} d_{nq} + v_q \end{aligned}, \tag{4-1}$$

which are similar in form to the generic linear time invariant system

$$a\dot{x} + bx = u$$

such that the following can be defined

$$\begin{aligned} u_d &= L_c \omega i_q - v_{dc} d_{nd} + v_d \\ u_q &= -L_c \omega i_d - v_{dc} d_{nq} + v_q \end{aligned} \tag{4-2}$$

By using the error signals $\tilde{i}_d = i_d^* - i_d$ and $\tilde{i}_q = i_q^* - i_q$, and applying proportional-integral compensation, we can choose d_{nd} and d_{nq} such that

$$\begin{aligned} u_d &= k_p \tilde{i}_d + k_i \int \tilde{i}_d dt \\ u_q &= k_p \tilde{i}_q + k_i \int \tilde{i}_q dt \end{aligned} \tag{4-3}$$

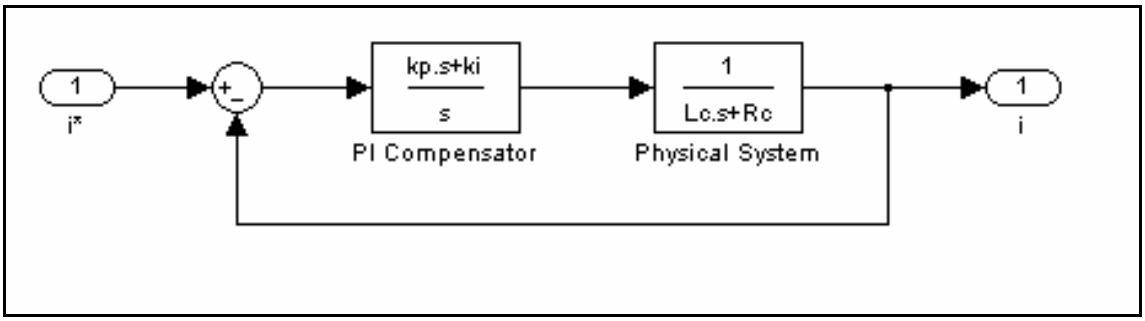

Figure 4.1 – Compensated Current Tracking Model

The transfer function of the proportional-integral compensator is

$$G_i(s) = \frac{U_q(s)}{\tilde{I}_q(s)} = \frac{U_d(s)}{\tilde{I}_d(s)} = k_p \frac{s + \frac{k_i}{k_p}}{s}, \tag{4-4}$$

and the closed loop transfer function of the current loop is

$$\frac{I_q(s)}{I_q^*(s)} = \frac{I_d(s)}{I_d^*(s)} = \frac{k_p}{L_c} \bullet \frac{s + \frac{k_i}{k_p}}{s^2 + \frac{R_c + k_p}{L_c} s + \frac{k_i}{L_c}} \tag{4-5}$$

Choosing $\zeta = \frac{\sqrt{2}}{2}$, we find that the overshoot of the system is 20.79%. Though significant, it is necessary in order to obtain the fastest response for the system. The resulting response is that of a second order LTI system. Thus,

$$k_p = 2\zeta\omega_{ni}L_c - R_c$$
$$k_i = L_c\omega_{ni}^2$$

Deriving the actual control inputs d_{nd} and d_{nq} via manipulation of the equations in (18), we arrive at

$$d_{nd} = \frac{v_d + L_c\omega i_q - u_d}{v_{dc}}$$
$$d_{nq} = \frac{v_q - L_c\omega i_d - u_q}{v_{dc}} \tag{4-6}$$

DC Voltage Control

To maintain some DC voltage level across the DC capacitor of the active power filter, the losses through the active filter's resistive-inductive branches can be compensated by acting on the supply current. Ideally, we want to act on the active current component i_d.

The equation for the DC voltage level in the model (3-15) is

$$C\frac{dv_{dc}}{dt} = d_{nd}i_d + d_{nq}i_q \tag{4-7}$$

We define our equivalent input as

$$u_{dc} = d_{nd}i_d + d_{nq}i_q \tag{4-8}$$

To regulate the DC voltage, the error

$$\tilde{v}_{dc} = v_{dc}^* - v_{dc}$$

is passed through the proportional-integral compensator

$$u_{dc} = k_1 \tilde{v}_{dc} + k_2 \int \tilde{v}_{dc} dt \,. \tag{4-9}$$

The resulting closed loop transfer function is

$$\frac{V_{dc}(s)}{V_{dc}^*(s)} = 2\zeta\omega_{nv} \frac{s + \frac{\omega_{nv}}{2\zeta}}{s^2 + 2\zeta\omega_{nv} s + \omega_{nv}^2}, \tag{4-10}$$

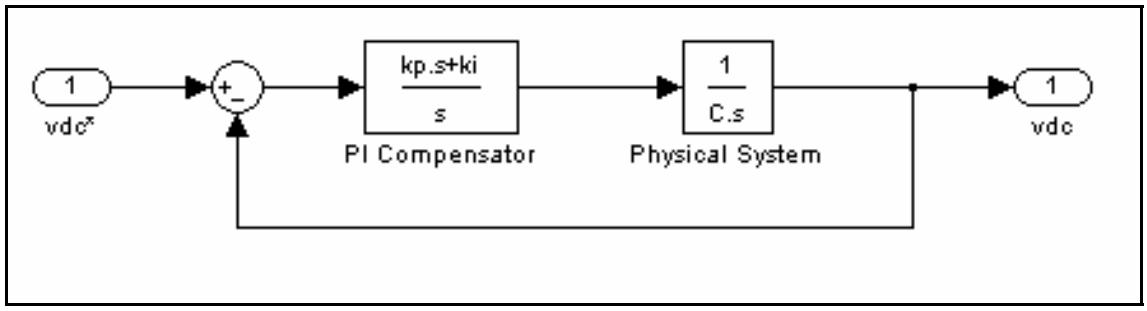

Figure 4.2 – Compensated Voltage Regulated Model

where the proportional and integral gains k_1 and k_2 are

$$\begin{aligned} k_1 &= 2\zeta\omega_{nv} C \\ k_2 &= \omega_{nv}^2 C \end{aligned} \tag{4-11}$$

Since we wish to use active current to maintain the DC capacitor voltage, we solve (4-8) for i_d to get

$$i_{d0}^* = \frac{u_{dc} - d_{nq} i_q}{d_{nd}} \tag{4-12}$$

Assuming normal operation of the active filter, the following properties can be observed

$$d_{nq} v_{dc} \approx v_q \text{ and } d_{nd} v_{dc} \approx v_d$$

Since we know that the supply voltages are

$$v_1 = \hat{V}\cos(\omega t)$$
$$v_2 = \hat{V}\cos(\omega t - \tfrac{2\pi}{3}) \quad ,$$
$$v_3 = \hat{V}\cos(\omega t - \tfrac{4\pi}{3})$$

and the transformation of the supply to the synchronous reference frame yields

$$\begin{bmatrix} v_d \\ v_q \end{bmatrix} = C_{dq}^{12}\begin{bmatrix} v_1 \\ v_2 \end{bmatrix} = \begin{bmatrix} \hat{V}\sqrt{\frac{3}{2}} \\ 0 \end{bmatrix} \tag{4-13}$$

Thus, the control effort is

$$i_{d0}^{*} = \frac{u_{dc} - d_{nq} i_q}{d_{nd}} = \frac{u_{dc} v_{dc} - d_{nq} v_{dc} i_q}{d_{nd} v_{dc}} = \sqrt{\frac{2}{3}}\frac{v_{dc}}{\hat{V}} u_{dc} \tag{4-14}$$

Control Inputs

In order to effectively utilize the harmonic current control law, we must provide it with an appropriate input signal to track. Ideally, we would choose periodic signals equivalent to the negated load current plus the fundamental harmonic. Such signals would approximate the necessary currents to be injected into the three-phase power system bus in order to compensate the generated harmonics out of the supply current. However, we can only approximate these signals from the existing load current and the angle of the voltage of each phase.

To accomplish this, we must rely on the properties of the synchronous rotating reference frame transformation described in equation (3-10). In particular, we must rely on the fact that a purely sinusoidal signal with frequency ω that is transformed to the synchronous rotating frame will yield a constant magnitude. In other words, we can apply a low-pass filter to the active component, i_d, of the synchronous rotating reference frame signals and subtract the

original signal to generate the appropriate tracking signal, i_d^*, for the active current controller. For the reactive component, i_q, we apply a negative gain to provide a control signal, i_q^* that not only tracks unwanted harmonics, but also the unwanted reactive component in the fundamental harmonic of the load currents.

It should be noted that this does not take into account the active current required to compensate for the parasitic resistances present in the voltage source inverter. Without such compensation, the voltage of the capacitor connected to the DC side of the voltage source inverter would decay. Thus, our need for DC voltage regulation, as described in Chapter III, arises. The additional active current required for this regulation is represented by the term i_{d0}^* in equation (4-14). Therefore, the resulting tracking signal for the active current component is $i_d^* + i_{d0}^*$, and the resulting tracking signal for the reactive current component is i_q^*, which is simply $-i_q$.

For our filter, we used a 4th-order low-pass filter with a cutoff frequency of roughly $\frac{\omega}{4\pi}$ (note that as described earlier, the DC component represents the fundamental).

The control input for the DC voltage regulation control loop is simply some predefined constant chosen to ensure that the DC capacitor is able to source an adequate amount of current without being driven to zero potential.

Compensating Current Synthesis

In order to synthesize the current necessary to cancel out unwanted harmonics in the supply current of a three-phase power system, we transform the synchronous rotating

reference frame into the stationary reference frame, and then perform space vector modulation on the stationary reference frame vector. This is necessary because the voltage source inverter can only represent eight discrete vectors, two of which have no effect on the injected current and the other six represented below in Figure 4. The two vectors that do not contribute to the injected current are located at the origin.

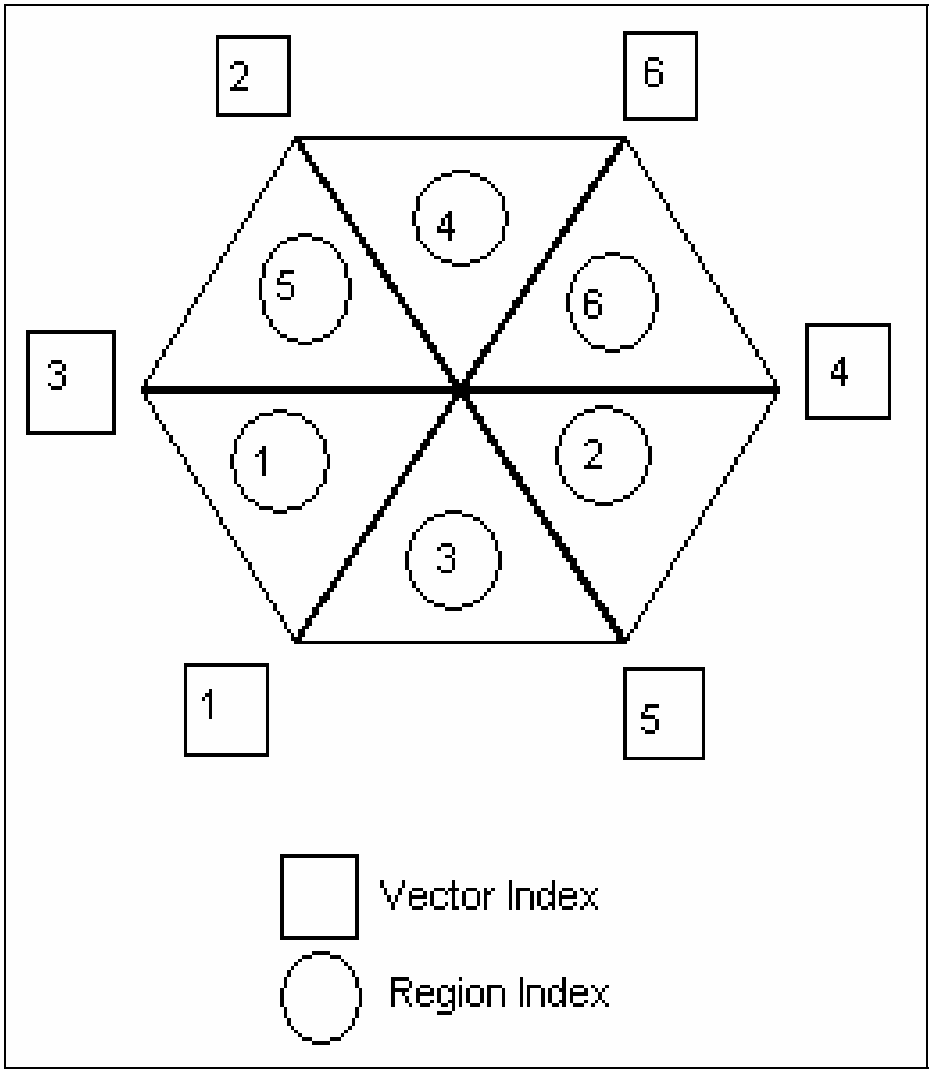

Figure 4.3 – Space Vectors for a Voltage Source Inverter in the Stationary Reference Frame

As can be seen, these vectors all have constant magnitude and angles. It may be the case that the vector that represents our desired injected current has an angle that is between two of these discrete vectors and may have a variable magnitude. Modulation of our desired vector allows us to represent it as the sum of fractions of these discrete vectors, as illustrated in Figure 4.4.

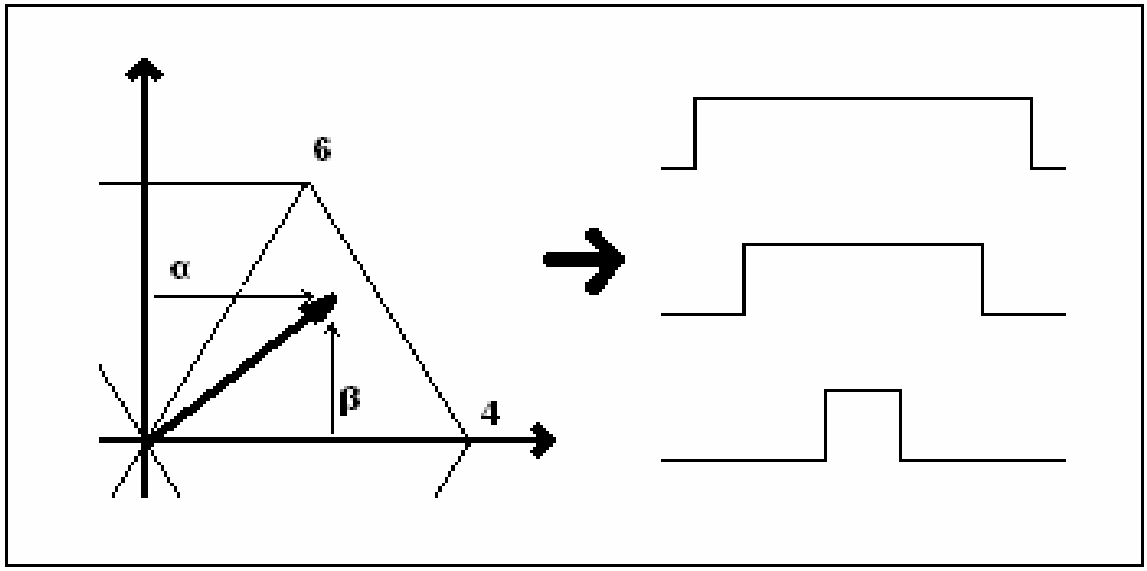

Figure 4.4 – Space Vector Modulation

The resulting PWM signal from our space vector modulation of the desired current vector is then applied directly to the switching signal inputs of our voltage source inverter. Note that a situation may occur where the vector representative of the current needed to adequately compensate the system may have a magnitude exceeding that capable of being represented by modulating the existing eight discrete space vectors. When this case occurs, the resulting modulated signal will represent a vector with a direction the same as the desired

vector, but will have a magnitude equivalent to the radius of a circle inscribed on the hexagonal boundary defined by the six effective discrete space vectors as shown in Figure 4.3.

Simulation Results

Simulation of the Proportional-Integral compensated shunt active power filter was implemented in MATLAB Simulink. Custom models were created in order to provide space vector modulated PWM signals with deadtime insertion necessary for the correct operation with switching elements modeled with realistic on and off times. However, in the simulations put forth in this thesis, we observe the special case of an ideal switch, which requires no deadtime insertion.

In our simulation, the total harmonic distortion of the current generated by the load is observed to be approximately 27.18%, whereas our compensated supply current has a total harmonic distortion of approximately 1.42% at steady state. A graphical representation of both the compensated and uncompensated harmonics is illustrated in Figure 4.5 and Figure 4.6

In Figure 4.7, we can see the actual supply voltages V1, V2, and V3, load currents I1, I2, and I3, filter currents If1, If2, and If3, supply currents Is1, Is2, and Is3, and the DC capacitor voltage Vdc that occurs in the compensated system. From top to bottom, they are supply voltage, load current, filter current, DC capacitor voltage, and compensated supply current. These waveforms represent an initial transition from an off state to an on state for the entire system on into steady state. Note that the DC capacitor voltage has an initial state of 350V, requiring that it be pre-charged to this voltage before operation of the active power filter in a real world application.

A simulation of the step response of the PI compensated system as it is switched from one load to another can be observed in Figure 4.8. In this simulation, the load is switched at steady state from a load consisting of a single resistive inductive branch of 15 Ohms and 5 mH to a load consisting of two resistive inductive branches, the first with a resistance of 15 Ohms and an inductance of 5 mH and the second with a resistance of 7.5 Ohms and 2.5 mH. Note the distortion that occurs in the signal during the step response transient before it reaches steady state.

Also note that the applied step change to the load of the system places the system into a mode where it is operating at limits imposed on it by both the saturation limit of the space vector used in the space vector PWM algorithm and the steady state voltage of the DC capacitor. It is conceivable to conclude that the resulting transient distortion is due to the overshoot of the PI compensated system and the fact that it is operating in a region well outside of the reasonable operational limits of the active power filter.

.

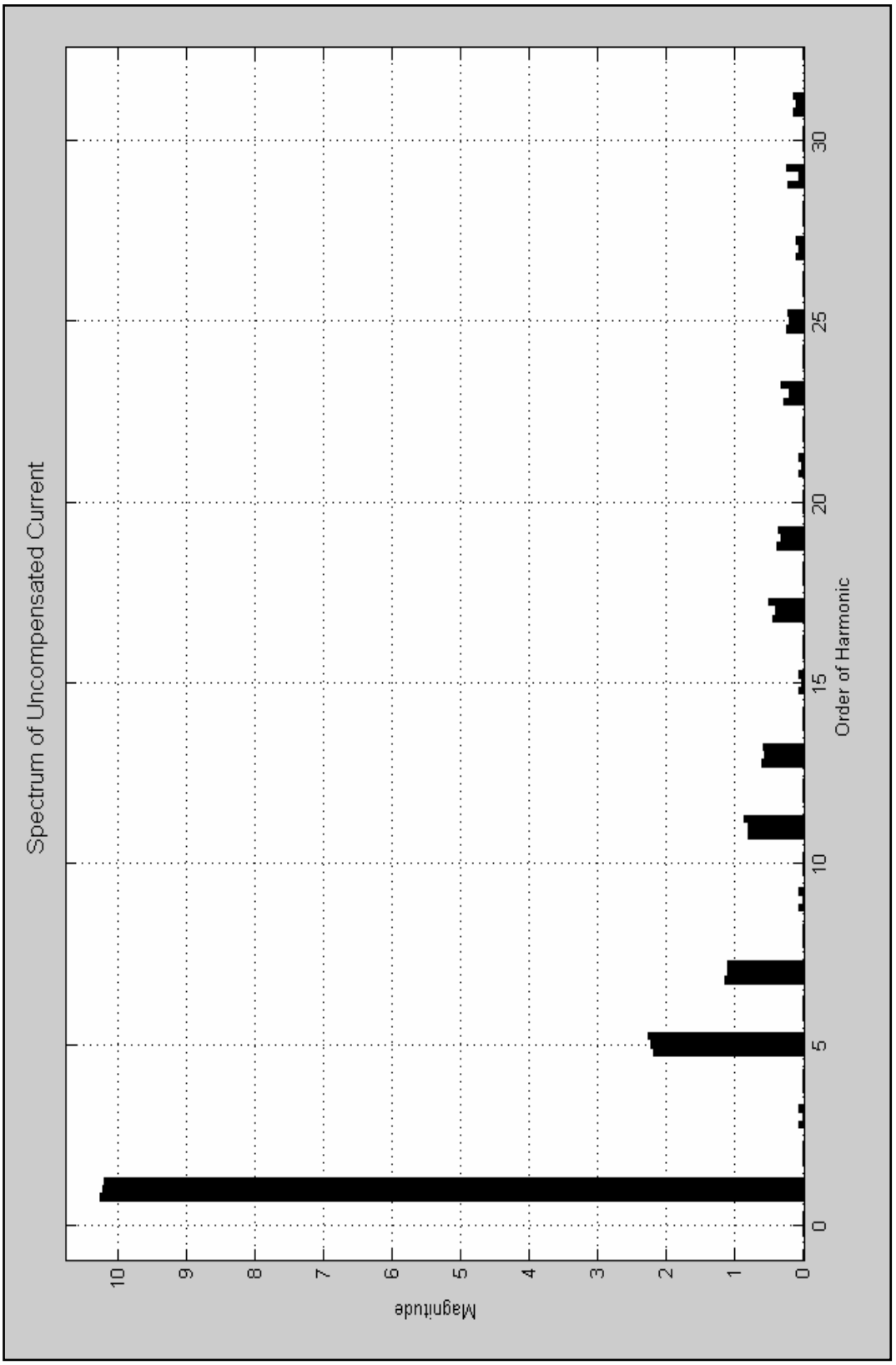

Figure 4.5 – Uncompensated Harmonic Currents and Fundamental

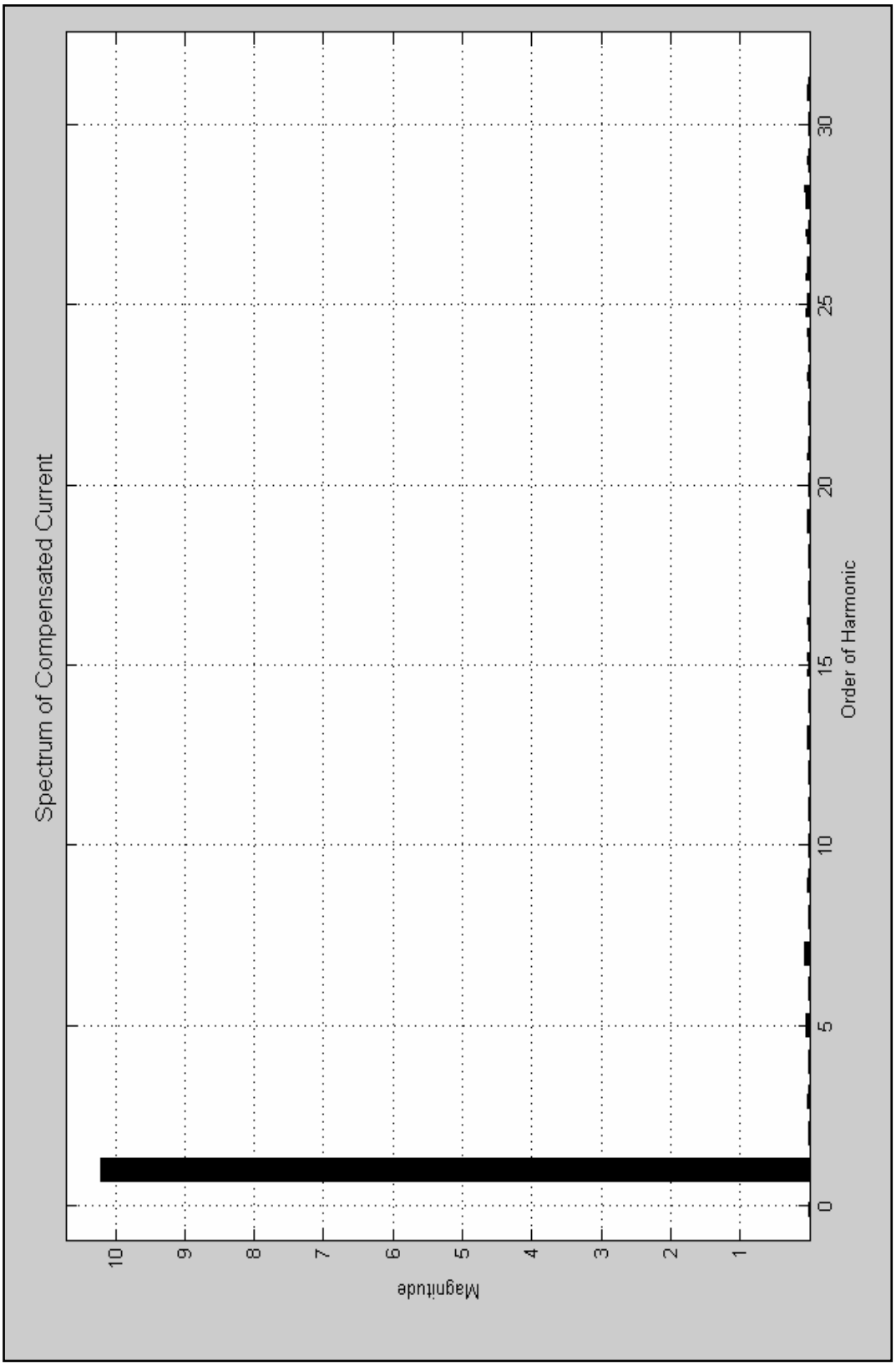

Figure 4.6 – PI Compensated Harmonic Currents and Fundamental

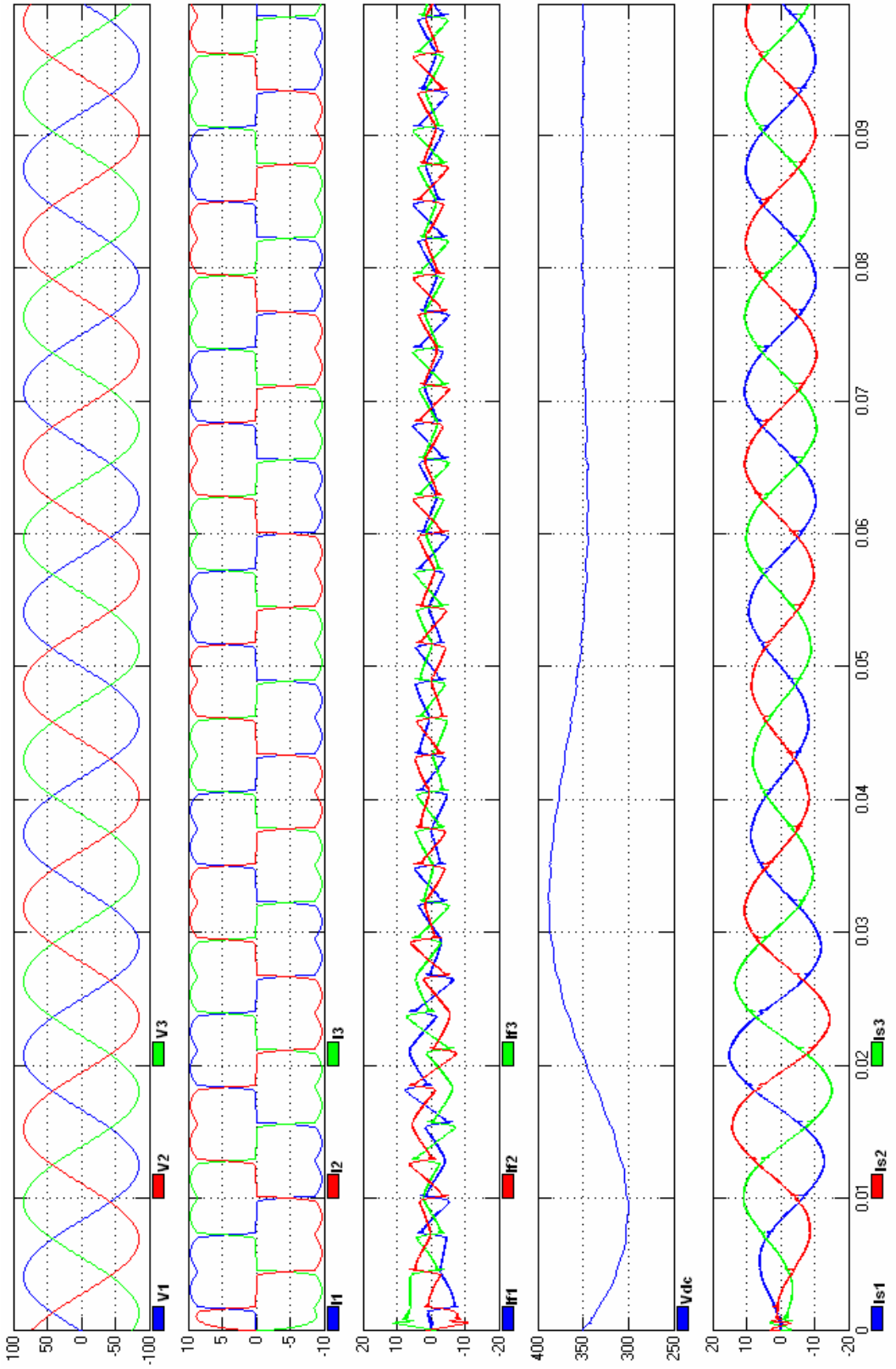

Figure 4.7 – Voltages and Currents in PI Compensated System

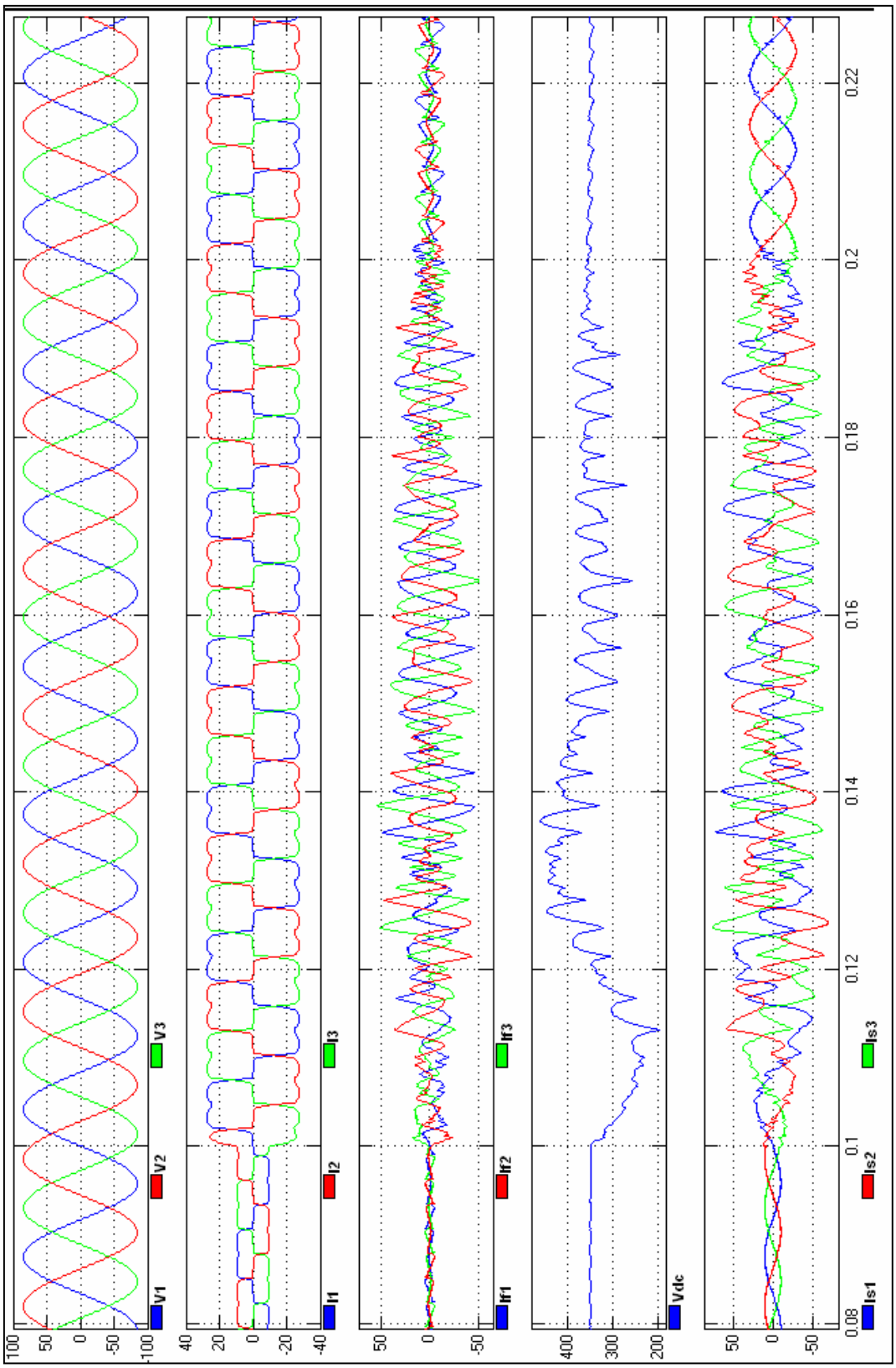

Figure 4.8 – Step Response of PI

CHAPTER V

SLIDING COMPENSATION OF AN ACTIVE POWER FILTER

A sliding mode controller was derived assuming that the state space of the shunt active power filter model consists of the synchronous rotating reference frame currents, i_d and i_q, and the DC voltage of the capacitor, v_{dc}. Much like the currents in the proportional-integral compensation discussed earlier, the currents i_d and i_q track the harmonic references extracted from the load currents as described in Chapter IV. The DC capacitor voltage is also regulated at a fixed value, again described in Chapter IV. The rate of convergence of these variables is directly dependent on the appropriate selection of sliding mode parameters.

Sliding Mode Switching Function

The property of a sliding mode controller that makes it an attractive option is the existence of a curve that approximates a control law, usually of lower order than the system it is designed for, in the phase plane or space towards which all external trajectories "slide" towards. These external trajectories are generally considered to exist on a "sliding surface" because of this property.

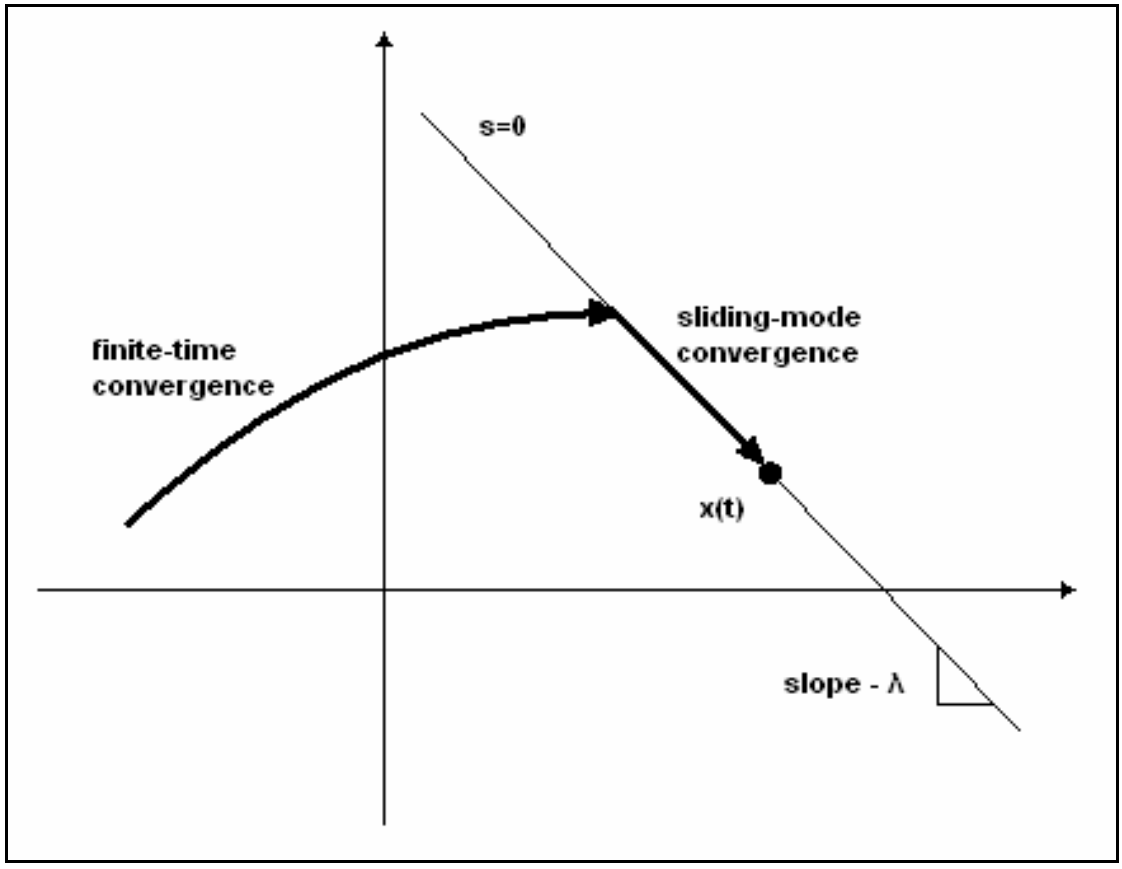

Figure 5.1 – Sliding Surface and Outside Trajectories

A control law for such a system is normally represented by an equation of the form $u = \hat{u} - k\,\mathrm{sgn}(s)$, where $\hat{u}$ approximates a control law where the net change of our sliding surface is zero and $-k\,\mathrm{sgn}(s)$ represents the sliding mode switching function that pulls trajectories towards the sliding surface. Note that the parameter s in the sliding mode switching function is also the sliding surface in question.

A sliding surface s is proposed by N. Mendalek et al in [2] as follows:

$$s = \begin{bmatrix} s_d \\ s_q \end{bmatrix} = \begin{bmatrix} k_1\left(x_1 - x_1^*\right) + k_2\left(x_3 - x_3^*\right) \\ k_1\left(x_2 - x_2^*\right) + k_3\left(x_3 - x_3^*\right) \end{bmatrix} \tag{5-1}$$

with $x^* = \begin{bmatrix} x_1^* & x_2^* & x_3^* \end{bmatrix}^T = \begin{bmatrix} i_d^* & i_q^* & v_{dc}^* \end{bmatrix}^T$ as the state space reference vector. From this, it can be seen that k_1 is directly applied to the error signals of the currents i_d and i_q whereas k_2 and k_3 are only indirectly related to said currents insofar as what current is necessary to regulate the capacitor voltage v_{dc} in the face of the parasitic resistances present in the voltage source inverter. Knowing this, we can show that $s = K\left(\mathbf{x} - \mathbf{x}^*\right)$ where

$$K = \begin{bmatrix} k_1 & 0 & k_2 \\ 0 & k_1 & k_3 \end{bmatrix} \tag{5-2}$$

Sliding Surface Stability

To ensure stability of the sliding surface over the entire state space of the system, and therefore ensure that the system converges to the control law curve $\hat{u}$, we must show that a Lyapunov function of s is strictly positive definite, its derivative is negative definite, and that the function approaches infinity as the magnitude of s itself approaches infinity. For this, we choose our Lyapunov function of s to be

$$V(s) = \frac{1}{2} s^T s \tag{5-3}$$

It can be seen that (5-3) is indeed strictly positive definite, meeting our first condition. It is also radially unbounded, satisfying our last condition. Taking the derivative of this, we arrive at

$$\dot{V}(s) = s^T \dot{s} \tag{5-4}$$

Where

$$\dot{s} = K(\dot{\mathbf{x}} - \dot{\mathbf{x}}^*)$$

$$= K\left(\begin{bmatrix} -\frac{R_c}{L_c} & \omega & 0 \\ -\omega & -\frac{R_c}{L_c} & 0 \\ 0 & 0 & 0 \end{bmatrix}\begin{bmatrix} x_1 \\ x_2 \\ x_3 \end{bmatrix} + \begin{bmatrix} -\frac{x_3}{L_c} & 0 \\ 0 & -\frac{x_3}{L_c} \\ \frac{x_1}{C} & \frac{x_2}{C} \end{bmatrix}\left(\hat{u} - k\,\mathrm{sgn}(s)\right) + \begin{bmatrix} \frac{v_d}{L_c} \\ \frac{v_q}{L_c} \\ 0 \end{bmatrix}\right) - K\dot{\mathbf{x}}^*$$

$$= \begin{bmatrix} k_1 & 0 & k_2 \\ 0 & k_1 & k_3 \end{bmatrix}\begin{bmatrix} -\frac{x_3}{L_c} & 0 \\ 0 & -\frac{x_3}{L_c} \\ \frac{x_1}{C} & \frac{x_2}{C} \end{bmatrix}\begin{bmatrix} -k\,\mathrm{sgn}(s_d) \\ -k\,\mathrm{sgn}(s_q) \end{bmatrix}$$

Further simplifying the derivative of the Lyapunov function, we find that we must select the elements of K such that the following inequality holds, satisfying the second condition necessary for convergence of all trajectories to the equivalent control law, $\hat{u}$.

$$-k_1 x_3 + \frac{L_c x_1\,\mathrm{sgn}(s_d) + x_2\,\mathrm{sgn}(s_q)}{C s_d\,\mathrm{sgn}(s_d) + s_q\,\mathrm{sgn}(s_q)}\left(k_2 s_d + k_3 s_q\right) < 0 \tag{5-5}$$

Equivalent Control

To determine the equivalent control law, $\hat{u}$, we reexamine the equation

$$\dot{s} = K(\dot{\mathbf{x}} - \dot{\mathbf{x}}^*) = K(A\mathbf{x} + B(\mathbf{x})\hat{\mathbf{u}} + G) - K\dot{\mathbf{x}}^* = 0 \tag{5-6}$$

Solving for $\hat{\mathbf{u}}$ gives us

$$\hat{\mathbf{u}} = -\left(KB(\mathbf{x})\right)^{-1} K\left(A\mathbf{x} + G - \dot{\mathbf{x}}^*\right) \tag{5-7}$$

Where $-(KB(\mathbf{x}))$ and $K\left(A\mathbf{x} + G - \dot{\mathbf{x}}^*\right)$ are defined as follows

$$\left(KB(\mathbf{x})\right)=\frac{-1}{-k_1\frac{x_3}{L_c}\left(-k_1\frac{x_3}{L_c}+k_2\frac{x_1}{C}\right)}\begin{bmatrix}-k_1\frac{x_3}{L_c} & -k_2\frac{x_2}{C}\\ 0 & -k_1\frac{x_3}{L_c}+k_2\frac{x_1}{C}\end{bmatrix} \tag{5-8}$$

$$K\left(A\mathbf{x}+G-\dot{\mathbf{x}}^*\right)=\begin{bmatrix}-k_1\frac{R_c x_1}{L_c}+k_1\omega x_2+k_1\frac{v_d}{L_c}-k_1\dot{x}_1^*\\ -k_1\omega x_1-k_1\frac{R_c}{L_c}x_2-k_1\dot{x}_2^*\end{bmatrix} \tag{5-9}$$

The resulting product, which incidentally are the coordinates of the equivalent control are

$$\begin{bmatrix}\hat{u}_d\\ \hat{u}_q\end{bmatrix}=\begin{bmatrix}\frac{k_1\left(-\frac{R_c}{L_c}x_1+\omega x_2+\frac{v_d}{L_c}-\dot{x}_1^*\right)}{-k_1\frac{x_3}{L_c}+k_2\frac{x_1}{C}}-\frac{k_2\frac{x_2}{C}\left(\omega x_1+\frac{R_c}{L_c}x_2+\dot{x}_2^*\right)}{\frac{x_3}{L_c}\left(-k_1\frac{x_3}{L_c}+k_2\frac{x_1}{C}\right)}\\ \frac{L_c}{x_3}\left(\omega x_1+\frac{R_c}{L_c}x_2+\dot{x}_2^*\right)\end{bmatrix} \tag{5-10}$$

Compensating Current Synthesis

Synthesis of the compensating currents for the sliding mode compensated shunt active power filter is done in the same fashion as that described in the Compensating Current Synthesis section in Chapter IV of this thesis.

Simulation Results

As with the simulation of the PI compensated active power filter, the sliding mode compensated active power filter simulation was implemented in MATLAB Simulink, and it was also assumed that it would operate in the special case of an ideal switch, which requires no deadtime insertion. Two different simulations of the sliding mode compensated system were performed, one with a hard non-linear switching element used to represent the sgn() function

necessary for finite-time convergence of the system state to the defined sliding surface, and another with a continuous approximation of a small area around the sliding surface in order to alleviate the switching chatter characteristic of sliding mode compensators with hard non-linear sgn() elements.

In the first simulation of the sliding mode compensated system, the total harmonic distortion of the current generated by the load is observed to be approximately 27.18%, whereas our compensated supply current has a total harmonic distortion of approximately 11.31% at steady state. A graphical representation of both the compensated and uncompensated harmonics is illustrated in Figure 5.2 and Figure 5.3.

In Figure 5.4, we can see the actual voltages and currents that occur in the sliding mode compensated system. From top to bottom, they are supply voltage, load current, filter current, DC capacitor voltage, and compensated supply current. These waveforms represent an initial transition from an off state to an on state for the entire system on into steady state. As in the PI Compensated system, the DC capacitor voltage has an initial state of 350V, requiring that it be pre-charged to this voltage before operation of the active power filter in a real world application.

A simulation of the step response of the sliding mode compensated system as it is switched from one load to another can be observed in Figure 5.5. Just as it was in the PI compensated system simulation, the load is switched in the sliding mode simulation at steady state from a load consisting of a single resistive inductive branch of 15 Ohms and 5 mH to a load consisting of two resistive inductive branches, the first with a resistance of 15 Ohms and an inductance of 5 mH and the second with a resistance of 7.5 Ohms and 2.5 mH. It can be noted that the distortion experienced in the PI compensated system does not occur in the

sliding mode compensated system. It is also apparent from the step response of both systems that the sliding mode system reaches steady state much sooner than the PI Compensated system.

As with the PI compensated system, the applied step change to the load of the system places it into a mode where the saturation limit of the space vector PWM algorithm and the steady state voltage of the DC capacitor are imposing limits on the effectiveness of the active power filter. Though the sliding mode compensated systems does not suffer the same transient distortion of the PI compensated system, the effects of these operation limits can be observed in the slight harmonic distortion present in the resulting compensated current waveform after steady state is reached.

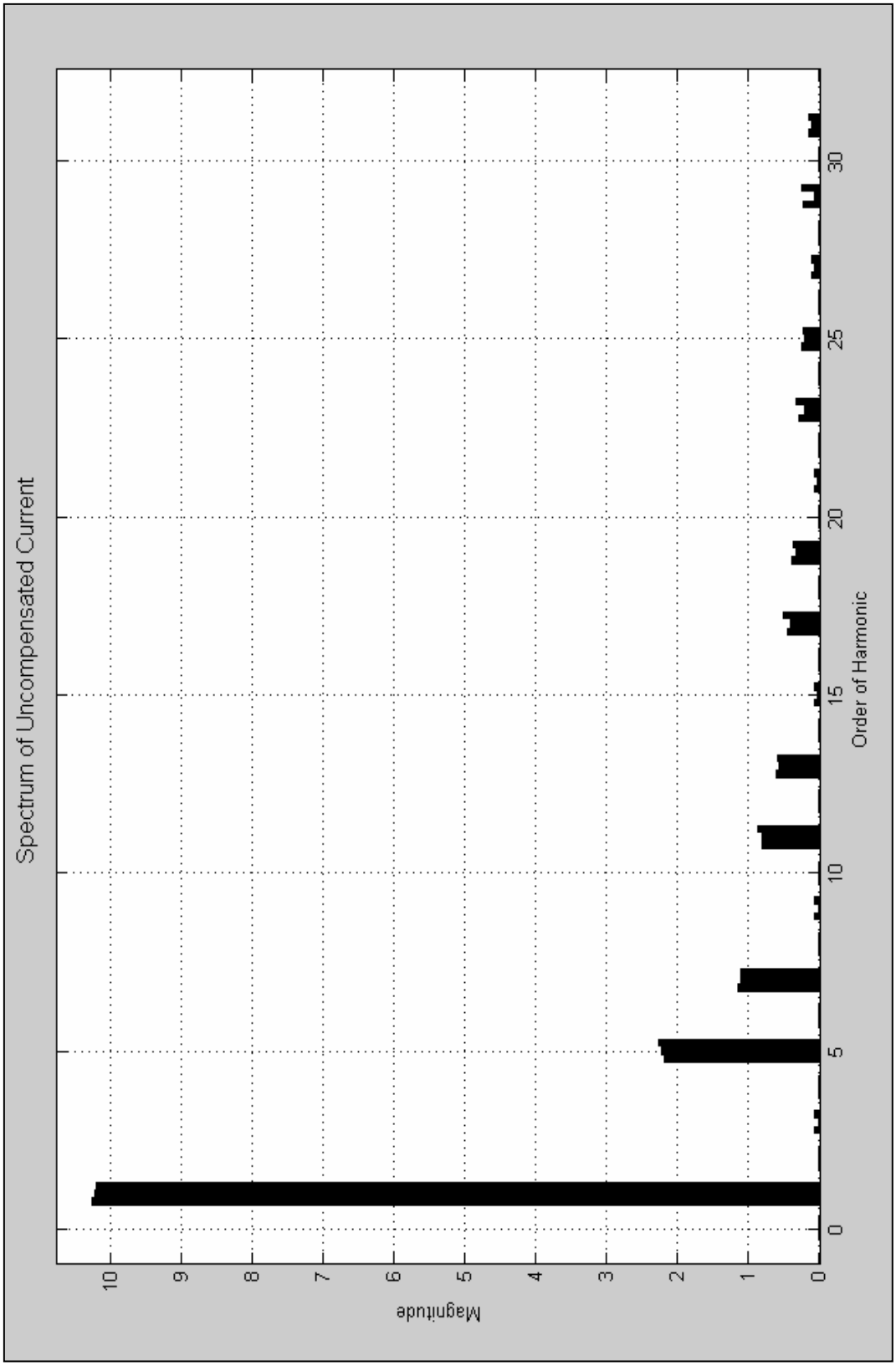

Figure 5.2 – Uncompensated Current for Sliding Mode

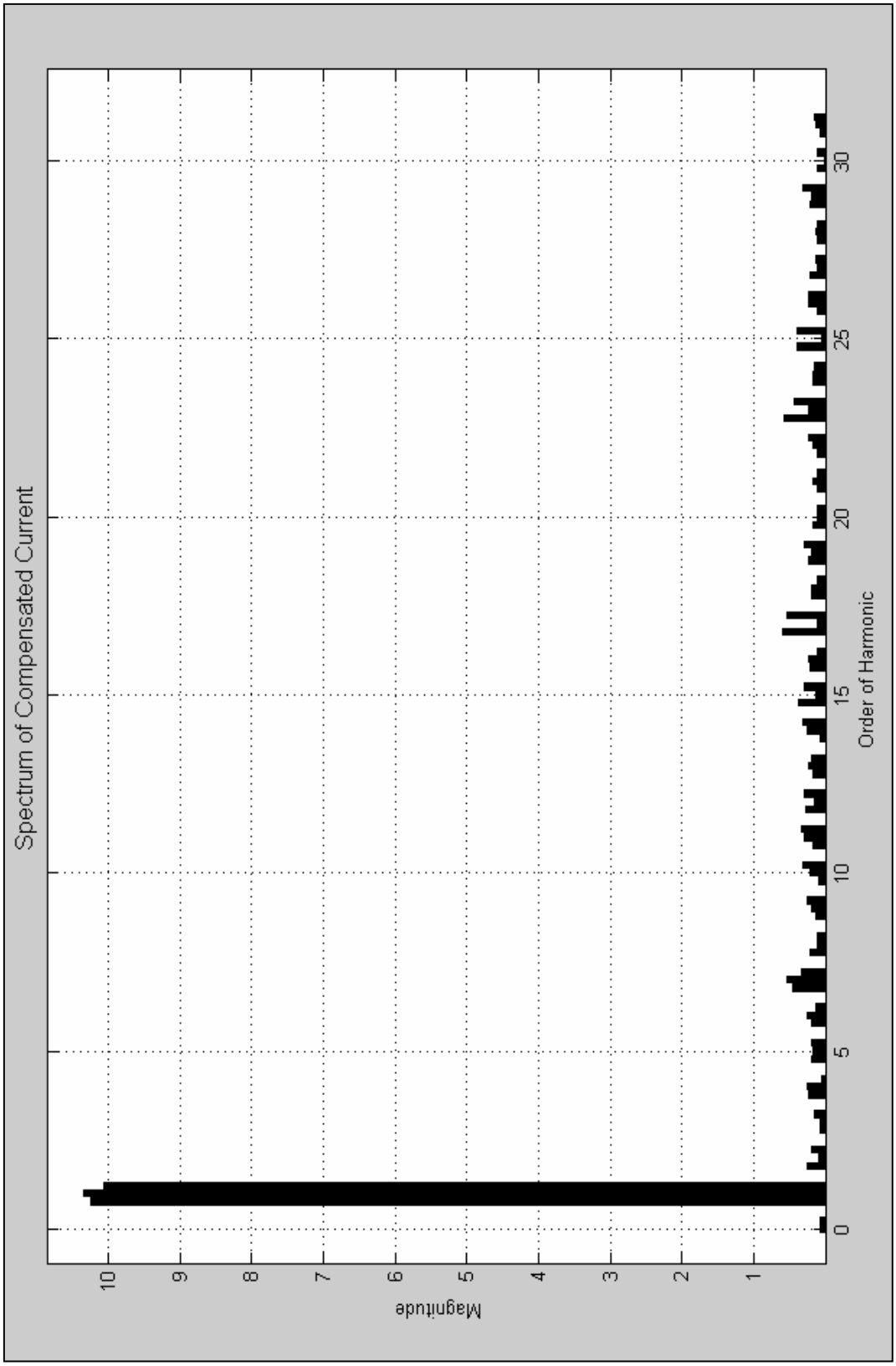

Figure 5.3 – Compensated Current for Sliding Mode

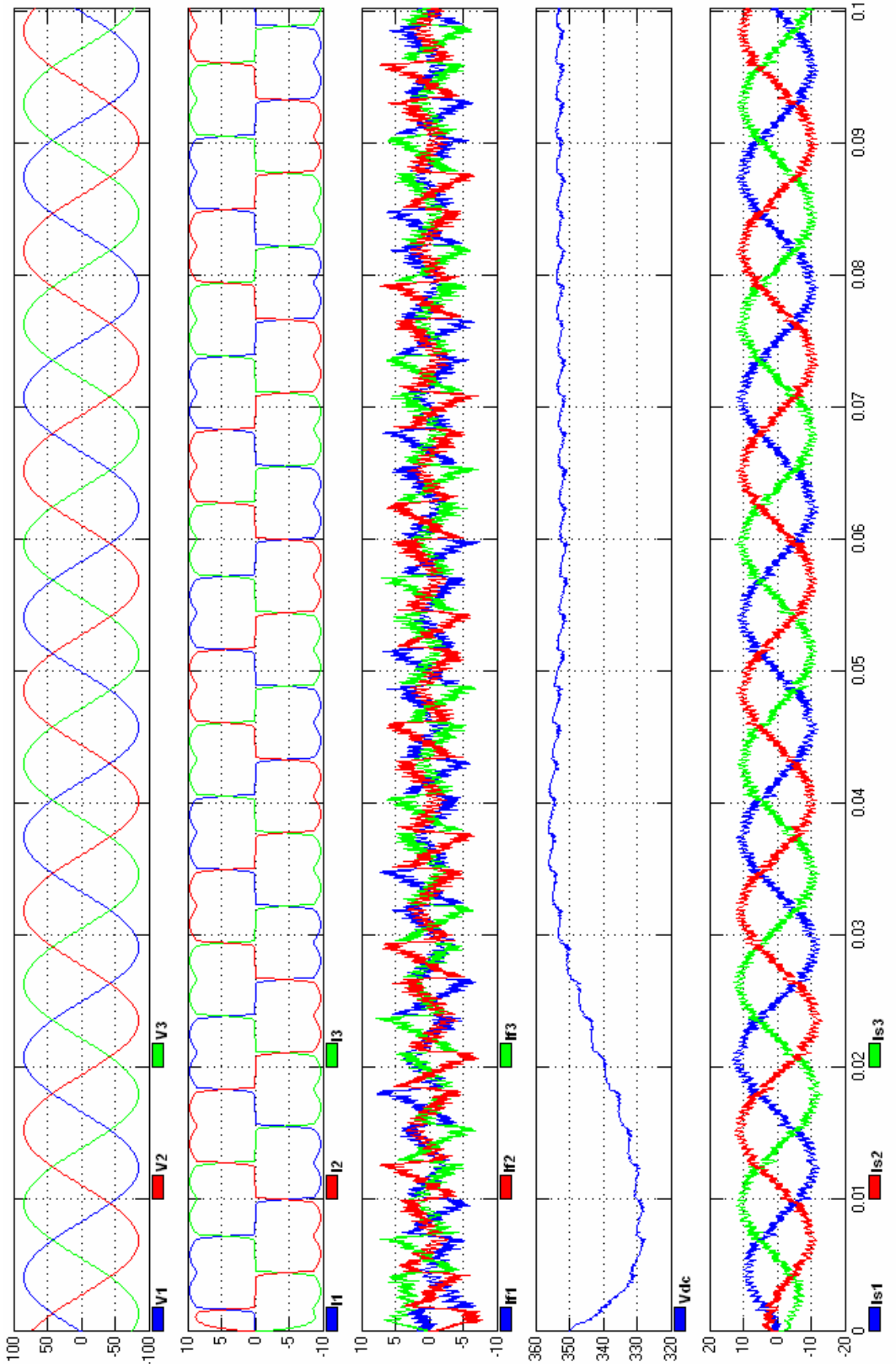

Figure 5.4 – Voltages and Currents in Sliding Mode System

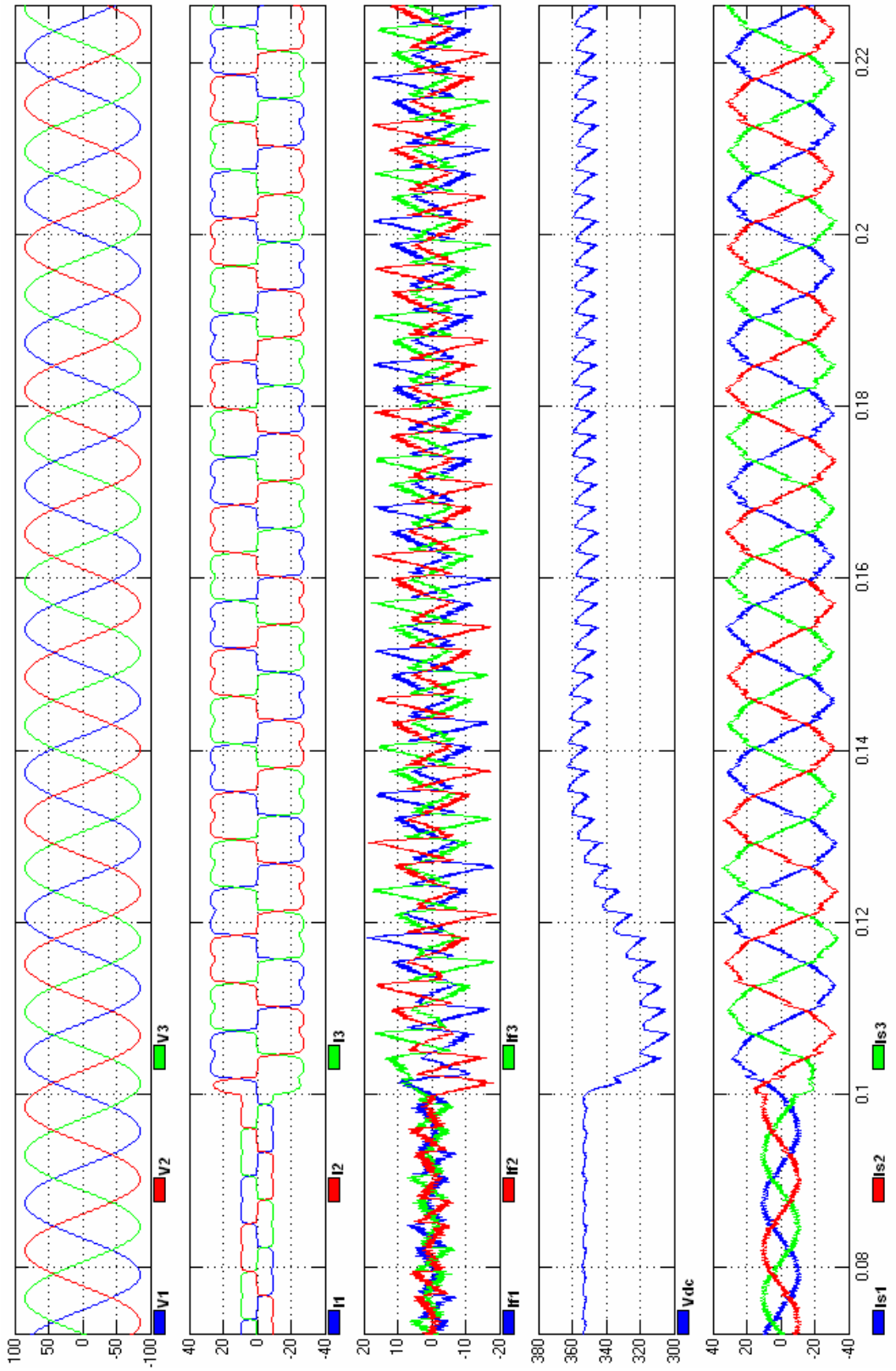

Figure 5.5 – Step Response of the Sliding Mode System

In the second simulation of the sliding mode compensated system, the total harmonic distortion of the current generated by the load is observed to be approximately 27.18%, whereas our compensated supply current has a total harmonic distortion of approximately 4.00% at steady state. A graphical representation of both the compensated and uncompensated harmonics is illustrated in Figure 5.6 and Figure 5.7.

In Figure 5.8, we can see the time domain representation of the voltages and currents that occur in the simulation of the sliding mode compensated system. From top to bottom, they are supply voltage, load current, filter current, DC capacitor voltage, and compensated supply current. These waveforms represent an initial transition from an off state to an on state for the entire system on into steady state. The DC capacitor voltage has an initial state of 350V, requiring that it be pre-charged to this voltage before operation of the active power filter.

A simulation of the step response of the sliding mode compensated system with continuous approximation of the sliding surface as it is switched from one load to another can be observed in Figure 5.9. The load is switched in the sliding mode simulation at steady state from a load consisting of a single resistive inductive branch of 15 Ohms and 5 mH to a load consisting of two resistive inductive branches, the first with a resistance of 15 Ohms and an inductance of 5 mH and the second with a resistance of 7.5 Ohms and 2.5 mH.

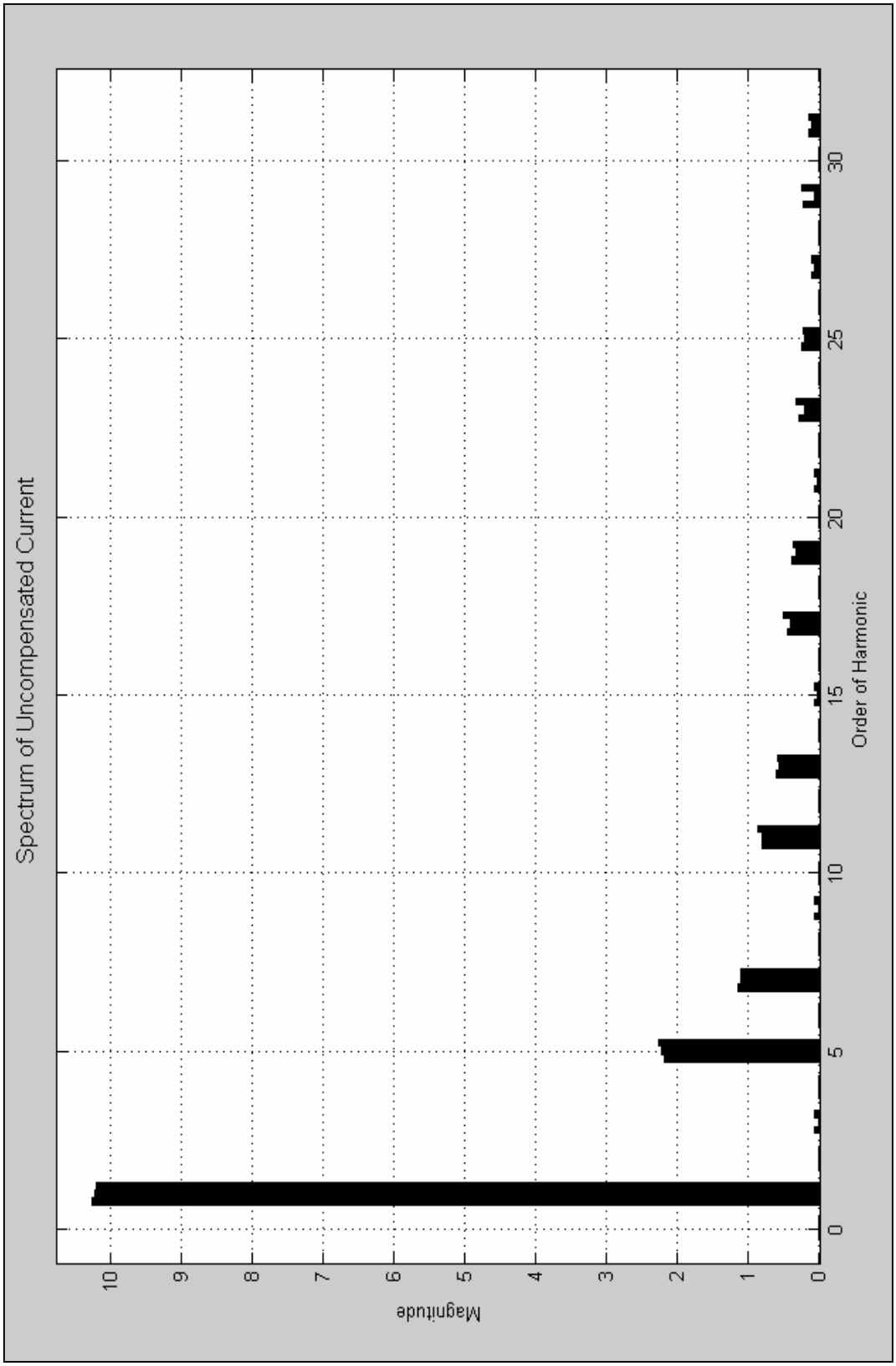

Figure 5.6 – Uncompensated Current for Sliding Mode with Continuous Approximation

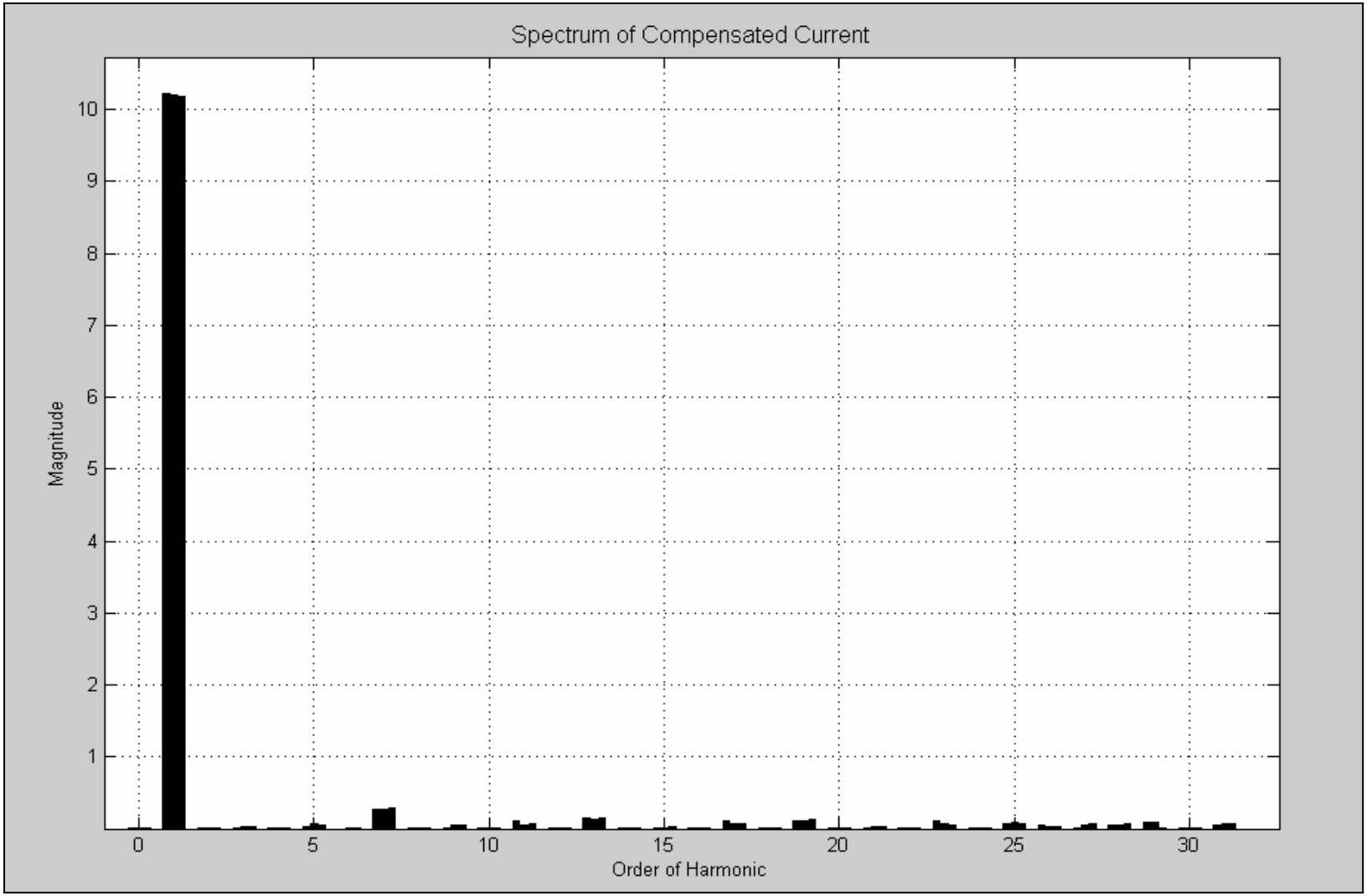

Figure 5.7 – Compensated Current for Sliding Mode with Continuous Approximation

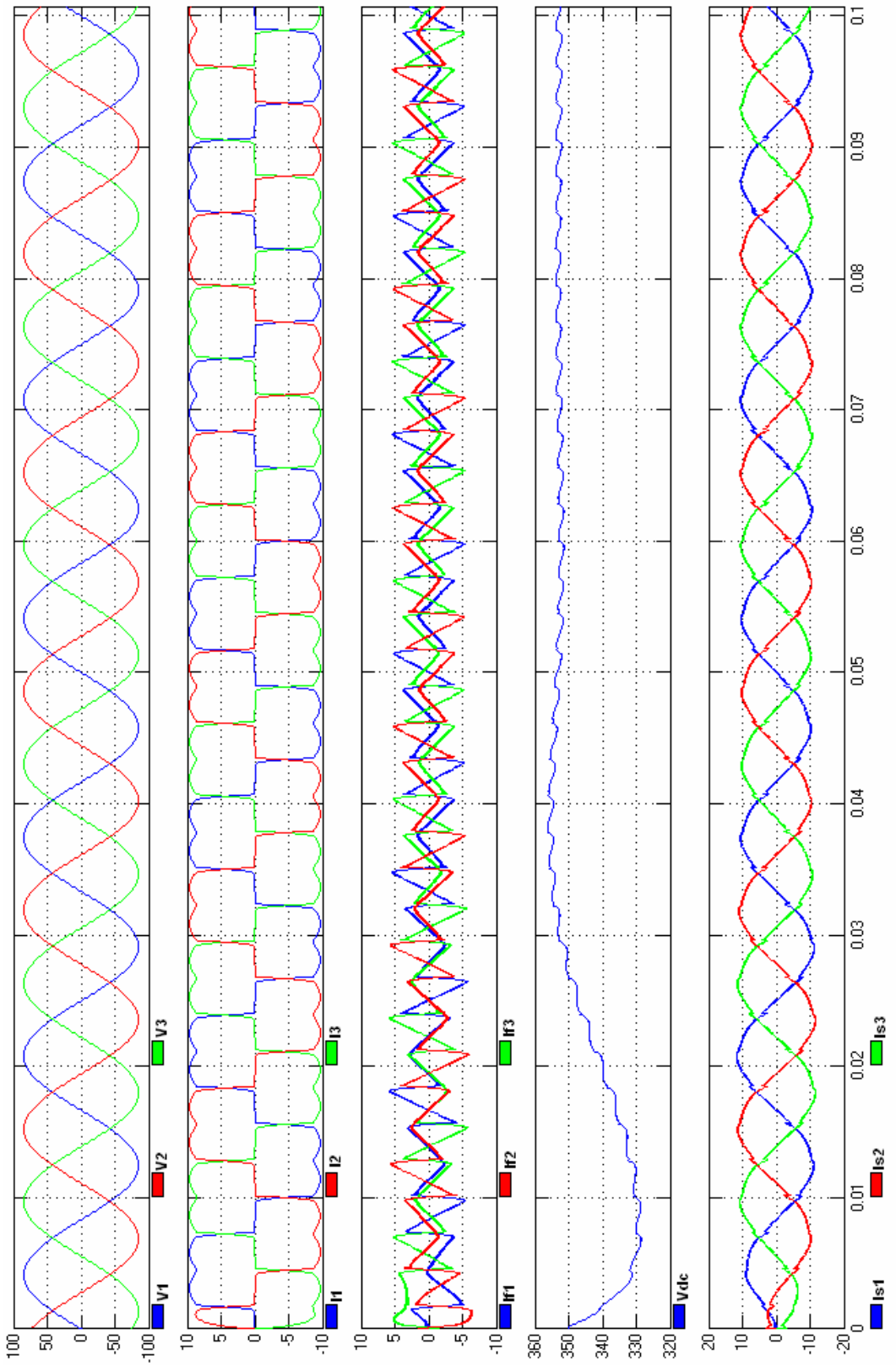

Figure 5.8 – Voltages and Currents in Sliding Mode System with Continuous Approximation

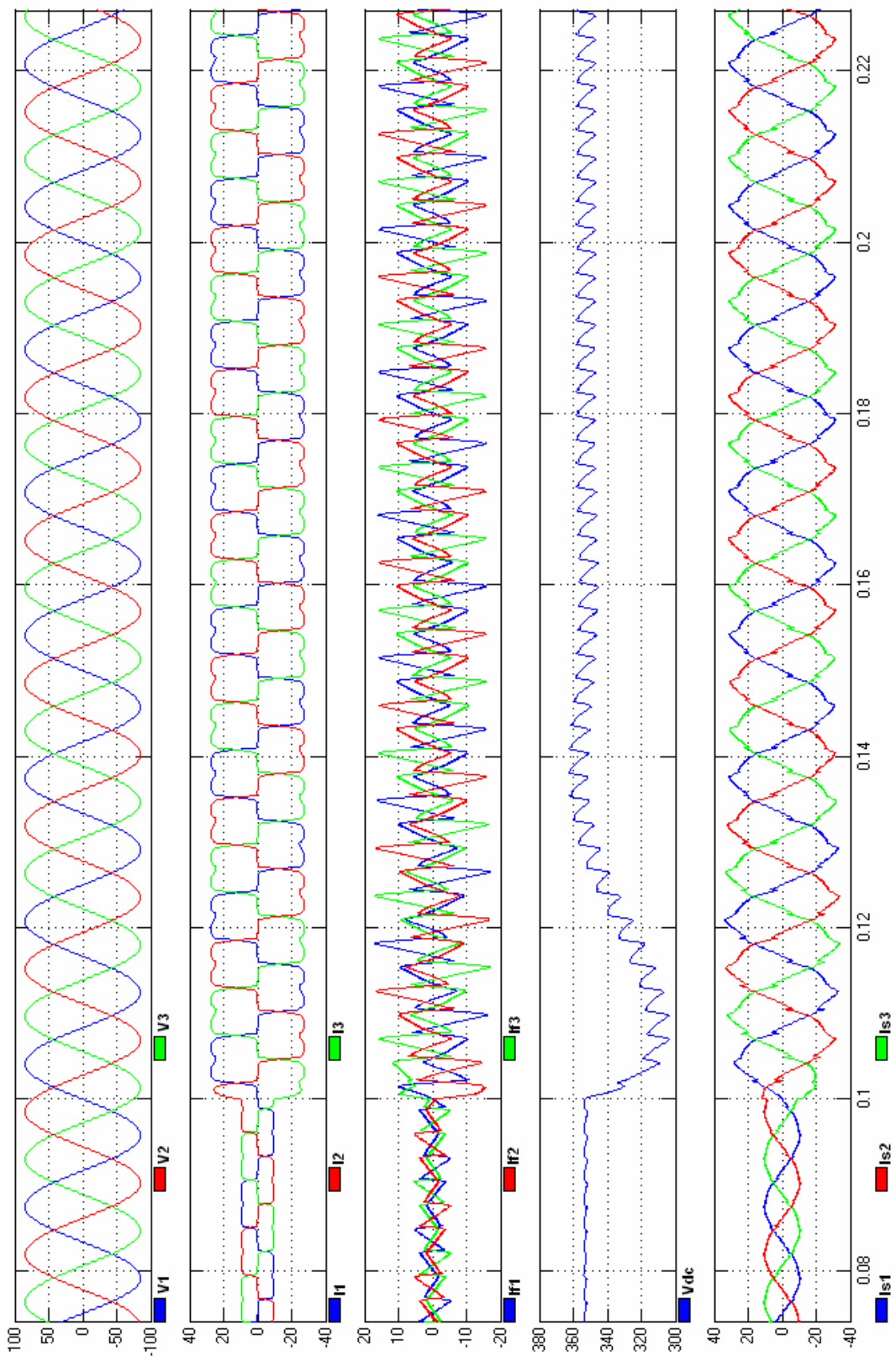

Figure 5.9 – Step Response of the Sliding Mode System with Continuous Approximation

CHAPTER VI

EVALUATION OF SIMULATION RESULTS

As can be seen from the simulation results, the two different classes of compensation techniques can have different advantages and disadvantages depending on their expected operating environment. The PI compensated active power filter results in significantly more acceptable THD levels at steady state, but suffers from a noticeable amount of overshoot when subjected to transient conditions. The sliding mode compensated active power filter results in higher THD levels than its PI compensated counterpart, but its behavior during transient conditions are not as volatile and tends to converge back to steady state much sooner. A set of possible scenarios where one or the other of these two compensation methods may be suitable can be seen in Table 1.

In either case, the THD in the current waveform of the compensated system is significantly better than the THD of an unfiltered current signal.

Table 6.1

HARMONIC FILTERING SCENARIOS

Scenario	Method	Reasoning
Diode bridge feeding a constant DC load.	Proportional-Integral	Provides cleanest current signal, and transient response can be neglected since load will rarely change.*
Thyristor controlled bridge feeding a variable rate DC motor. (Low Current)	Proportional-Integral	Provides cleanest current signal, and transient response can be neglected provided that current consumption of the load does not approach limits imposed by filter parameters.*
Thyristor controlled bridge feeding a variable rate DC motor. (High Current)	Sliding Mode	Provides a much more stable response when operating at or near the current limits imposed by filter parameters.*
IGBT Switched VSI inverter feeding a load with highly unpredictable transient conditions.	Sliding Mode	Provides a much more stable response to transient conditions provided that it is not operated beyond the current limits imposed by filter parameters.*

***Note: These parameters include the DC capacitor steady state voltage level.**

CHAPTER VII

CONSIDERATIONS AND LIMITATIONS

Through simulation, we have shown that the application of an active power filter to a power distribution system with unwanted harmonics can result in a relatively clean current waveform. However, the application of an active power filter in a real world application presents certain caveats that should be addressed. First and foremost, care should be taken into account in implementation of the phase lock-loop (PLL) used to synchronize the active power filter to the three-phase voltage waveform. In the simulation, a virtual PLL was used which would always guarantee an ideal phase angle synchronized to the voltage waveform. Unfortunately, real world PLL's are usually subject to some inherent jitter, injecting a certain amount of disturbance into the system. Additionally, distortion in the current waveforms will result in some distortion in the voltage waveforms. Since a real world PLL synchronizes itself to the voltage waveforms of the three-phase system, an additional feedback path exists in the system that may give rise to unpredictable behavior if not taken into account.

The fact that distortion can occur in the voltage waveforms gives rise to the requirement that the input to the PLL should be low-pass filtered in order to prevent unwanted distortion in the voltage signal from contributing to the jitter in the resulting PLL phase angle. The act of low-pass filtering this signal will result in a lag in the signal input into

the PLL, and will require an appropriate lag, lead, or lag-lead compensator in order to ensure that the input signal to the PLL is in phase with the distorted voltage waveforms.

The last major consideration to take into account is that of the capacitor connected to the DC side of the VSI in the active power filter. This capacitor must be pre-charged to a particular voltage prior to operation of the active power filter, normally to the voltage where it will typically remain during steady state of the active power filter's operation. This voltage determines not only the parameters of the capacitor selected, but also the maximum current capable of being injected into and absorbed from the power distribution system by the active power filter during operation without going into an unstable or unpredictable mode.

In all, the three major caveats are as follows:

- A real world PLL provides an additional feedback path into the system that should be taken into account.
- Real world voltage waveforms may contain distortion that make them unsuitable as inputs to a real world PLL, and should be appropriately low-pass filtered and compensated.
- The DC capacitor present in the system should be pre-charged to its steady state voltage level, which determines its rating and the maximum effectiveness of the active power filter.

CHAPTER VIII

CONCLUSIONS AND FURTHER WORK

In our simulations, we are able to make a reasonable comparison between proportional-integral and sliding mode compensated active power filtering devices. Their effectiveness in different environments leads us to believe that proportional-integral compensation active power filtering solutions are suited for static environments where environmental parameters would vary relatively slowly over time. Such an example would be a three leg diode bridge feeding a series of heater coils, essentially a load that will change very little over a significant period of time. On the other hand, sliding mode compensation active power filtering solutions are better suited for dynamic environments where the parameters of the load may have significant transient activity. A good example of this would be a three leg diode bridge feeding a DC motor operating at various mechanical loads and velocities in an indeterminate manner respective to the rest of the system.

However, our simulations do not take into account real world implementations of the same systems and the complexities such implementations would introduce. Further work on this topic could consist of the simulation of similarly compensated active power filters that more accurately reflect a potential real world implementation paired with a quantitative determination of the relationship between the steady state voltage of the DC capacitor present

in the system and the maximum current capable of being injected into and absorbed from the power distribution system.

BIBLIOGRAPHY

[1] J-J. Slotine, W. Li, *Applied Nonlinear Control,* Prentice Hall, 1991.

[2] N. Mendalek and K. Al-Haddad, "Modeling and Nonlinear Control of Shunt Active Power Filter in the Synchronous Reference Frame", IEEE ICHQP'2000, pp. 30-35, 2000.

[3] N. Mendalek, K. Al-Haddad, F. Fnaiech, and L. A. Dessaint, "Sliding Mode Control of 3-Phase 3-Wire Shunt Active Filter in the dq Frame", IEEE CCECE'2001, pp. 765-770, 2001.

[4] G.-Y.Jeong, T.-J.Park, and B.-H.Kwon, "Line-Voltage-Sensorless Active Power Filter for Reactive Power Compensation", IEE Proceedings-Electric Power Applications'2000, pp. 385-390, 2000.

[5] D. Rivas, L. Morán, J. Dixon, and J. Espinoza, "A Simple Control Scheme for Hybrid Active Power Filter", IEEE PESC'2000, pp. 991-996, 2000.

[6] D. Gao, "Designa and Performance of an Active Power Filter for Unbalanced Loads", IEEE PowerCon'2002, pp. 2496-2500, 2002.

[7] J. Dixon, L. Morán, "A Control System for a Three Phase Active Power Filter which Simultaneously Compensates Power Factor and Unbalanced Loads", IEEE IECON'1993, pp. 1083-1087, 1993.

[8] L. Morán, J. Dixon, "An Active Power Filter Implemented with PWM Voltage-Source Inverters in Cascade", IEEE ISIE'1994, pp. 108-113, 1994.

[9] C.A.Claro, J. Kaffka, A. Campos, "Analysis and Design of a Shunt Active Power Filter Employing a Dead Beat Control Technique", IEEE IECON'1999, pp. 1427-1433, 1999.

[10] D. Shen and P.W. Lehn, "Fixed-Frequency Space-Vector-Modulation Control for Three-Phase Four-Leg Active Power Filters", IEE Proceedings-Electric Power Applications'2002, pp. 268-274, 2002.

[11] S.-J. Huang and J.-C. Wu, "Design and Operation of Cascaded Active Power Filters for the Reduction of Harmonic Distortions in a Power System", IEE Proceedings-Generation Transmission and Distribution'1999, pp. 193-199, 1999.

[12] T. Kataoka, Y. Fuse, D. Nakajima, and S. Nishikata, "A Three-Phase Voltage-Type PWM Rectifier with the Function of an Active Power Filter", IEE Proceedings-Power Electronics and Variable Speed Drives'2000, pp. 386-391, 2000.

[13] E.H. Song and B.H. Kwon, "A Novel Digital Control for Active Power Filter", IEEE IECON'1992, pp. 1168-1173, 1992.

[14] M. Kurokawa, M. Rukonuzzaman, Y. Konishi, H. Iwamoto, and M. Nakaoka, "Space Voltage Vector Modulated Three-Phase Voltage Source Soft-Switching Active Power Filter", IEEE PEDS'1999, pp. 996-1002, 1999.

[15] D. Gao and X. Sun, "A Shunt Active Power Filter with Control Method Based on Neural Network", IEEE Powercon'2000, pp. 1619-1624, 2000.

[16] M. Kurokawa, Y. Konishi, C.Y. Inaba, and M. Nakaoka, "Space Voltage Vector Modulated Three-Phase Voltage Source Soft-Switching Active Power Filter for Next Generation FACTS", IEEE PES'2000, pp. 2459-2464, 2000.

[17] H.-H. Kuo, S.-N. Yeh, and J.-C. Hwang, "Novel Analytical Model for Design and Implementation of Three-Phase Active Power Filter Controller", IEE Proceedings-Electric Power Applications'2001, pp. 369-383, 2001.

[18] W.S. Oh, Y.T. Kim, and H.J. Kim, "Dead Time Compensation of Current Controlled Inverter using Space Vector Modulation Method", IEEE PEDS'1995, pp. 374-378, 1995.

[19] F. Blaabjerg, S. Freysson, H.-H. Hansen, and S. Hansen, "A New Optimized Space Vector Modulation Strategy for a Component Minimized Voltage Source Inverter", IEEE APEC'1995, pp. 577-585, 1995.

[20] G.D. Marques, "A PWM Rectifier Control System with DC Current Control Based on the Space Vector Modulation and AC Stabilisation", IEE Proceedings-Power Electronics and Variable Speed Drives'1998, pp. 74-79, 1998.

[21] K. Zhou and D. Wang, "Relationship Between Space-Vector Modulation and Three-Phase Carrier-Based PWM: A Comprehensive Analysis", IEEE Transactions on Industrial Electronics, Vol. 49, No. 1, pp. 186-196, 2002.